Exploring the Quantum Nature of Light with Compton Scattering

Sam Greydanus*
sam.17@dartmouth.edu

Abstract

Compton scattering occurs when a photon and an electron undergo a relativistic elastic scattering process. This process demonstrates the quantum nature of light in a dramatic way. To study Compton scattering in the laboratory, we introduce a scattering experiment which uses ^{137}Cs as a radiation source and aluminum as a target. We describe a calibration process which uses additional radiation sources, ^{60}Co and ^{22}Na. Next, we measure the effect of scattering angle on photon count and energy spectra. We show that the interaction requires relativistic calculation, in particular use of the Klein-Nishina formula.

1 Introduction

The Compton effect, first described by Arthur Compton in 1923 [1] is a classic example of the quantum nature of light. When an incident gamma ray interacts with a stationary electron, it will behave like a particle and scatter according to the physics of an elastic collision.

The ideal photon energy range for Compton scattering is around that of a the rest mass of an electron, which is 511 keV. When this is the case, the electron and photon have approximately the same amount of energy and scattering can occur. This experiment uses ^{137}Cs as a gamma ray source because it emits photons at 662 keV, quite close to the rest mass energy of an electron.

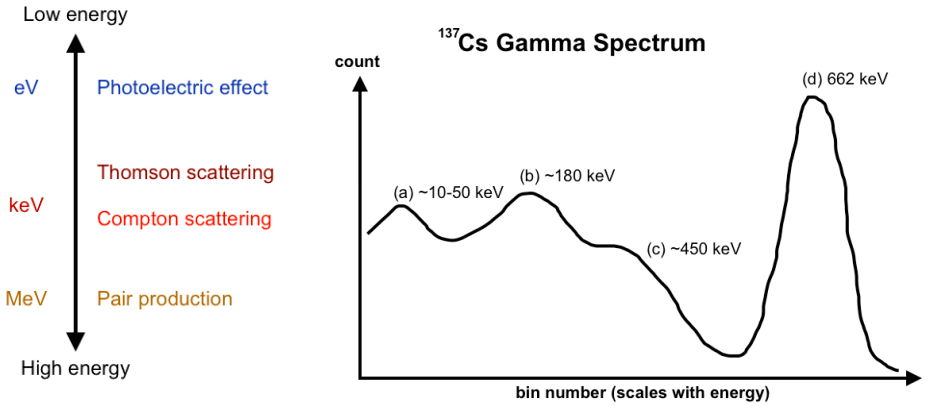

(a) Dominant photon-electron interactions for various energy regimes

(b) Sketch of energy spectrum of ^{136}Cs. a) electron bremsstahlung. b) Compton backscatter. c) Compton edge. d) radiation from ^{136}Cs.

Figure 1: ^{137}Cs is a good source for Compton scattering because it emits gamma rays at 662 keV, which is in the ideal energy range for Compton scattering [4]

*Worked with Ethan Isaacson.

2 Background

2.1 Scintillation detectors

Scintillators detect incident particles by converting their energy to visible light, then converting that light to electric current. In this experiment, we will use a scintillator with a NaI(TI) crystal. When gamma rays enter the detector, they deposit some or all of their energy on the electrons of the crystal. As these electrons are recaptured by their atoms, they emit visible light, which travels through the crystal to a photomultiplier tube. This tube produces a current proportional to the energy of the incident photon. An RC circuit transforms this small current into a voltage pulse which is also proportional to the original gamma ray's energy. Finally, a computer logs the information.

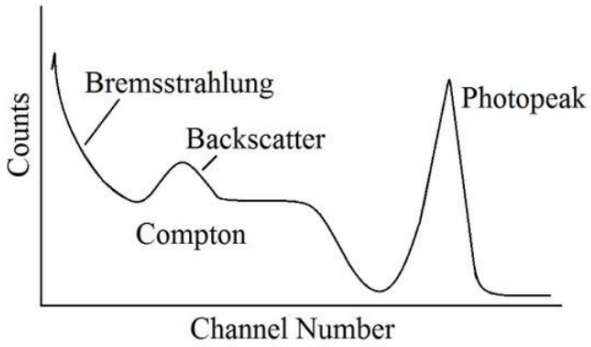

Figure 2: A typical measurement of photon counts versus channel number for the NaI(TI) scintillator. The photopeak corresponds to incident gamma rays which deposited *all* of their energy in the crystal.

Some of the original gamma rays deposit only a fraction of their total energy in the photomultiplier. This means that even if all of the incident gamma rays have approximately the same energy, the scintillator will measure a spectrum of energy such as Figure 2. During analysis, we will begin with photon counts across a broad range of energy spectra and look for photopeaks; photopeaks are important because they are directly proportional to the total energy of the incident gamma rays.

2.2 Theory of Compton scattering

The final energy of a photon with initial energy $h\nu_0$ that is scattered after an elastic collision with an electron at rest (where the collision occurs at angle θ) is given by:

$$h\nu = \frac{h\nu_0}{1 + (h\nu_0/mc^2)(1 - \cos\theta)} \tag{1}$$

Photons for which $h\nu_0$ is much larger than the binding energy of electrons in the atoms of the target material interact with bound electrons in the same way. Klein and Nishina (1929) [2] derived a formula (2 for the differential scattering cross section of these photons as a function of scattering angle.

$$\frac{d\sigma}{d\Omega} = r_0^2 \frac{1 + \cos^2\theta}{2[1 + \gamma(1 - \cos\theta)]^2} \times \left[1 + \frac{\gamma^2(1 - \cos\theta)^2}{(1 + \cos^2\theta)[1 + \gamma(1 - \cos\theta)]}\right] \tag{2}$$

where $\gamma = h\nu_0/mc^2$ and $r_0 = 2.818 \times 10^{-13}$ cm is the classical electron radius [4]. The Klein-Nishina formula (equation 2) is different from the formula for Thompson scattering. The equation for

Thompson scattering (equation 3) is actually a simplification of the Klein-Nishina formula, for cases where $h\nu \ll m_e c^2$, or, equivalently, $\gamma \ll 1$.

$$h\nu = r_0^2 \frac{1 + \cos^2 \theta}{2} \tag{3}$$

It is possible to verify this relationship experimentally. First, define the following quantities:

- N_0: number of photons incident on scatterer (per second)
- N: number of photons incident on detector (per second)
- $\Delta\Omega = 0.05$: solid angle subtended by counter at the scattering point
- $Z = 13$: atomic number of scattering atoms (Aluminum, in this case)
- $M = 4.4803895658 \times 10^{-26}$: molecular weight of scattering atoms
- $d = 0.01$: thickness of scattering material in the path of the beam (m)
- $\rho = 2700$: density of scattering material (kg/m^3)
- $\lambda = 6.02 \times 10^{23}$: Avogadro's number
- I: incident flux of photons
- n: number of scattering electrons in the scatterer in path of beam

These quantities relate to each other as follows

$$N = nI\left(\frac{d\sigma}{d\Omega}\right) \quad and \quad n = AdZ\frac{\rho\lambda}{M} \quad and \quad I = \frac{N_0}{A} \tag{4}$$

. Combining these terms, we have

$$N = N_0 \frac{d\sigma}{d\Omega}\left(\frac{dZ\rho\lambda}{M}\right) \tag{5}$$

Now, we can find $\frac{d\sigma}{d\Omega}$ experimentally by rearranging and dividing by $\Delta\Omega$:

$$\frac{d\sigma}{d\Omega} = \frac{N}{N_0}\left(\frac{M}{dZ\rho\lambda(\Delta\Omega)}\right) \tag{6}$$

2.3 Other considerations

First, the Klein-Nishna formula (equation 2) was derived for a thin scatterer. In this experiment, the scattering target will have a thickness on the order of 1 cm; it is a thick scatterer. This means that the data should be corrected for the absorption of the scattered radiation.

The scintillation detector will not only pick up radiation from the ^{137}Cs source, it will pick up radiation from the environment as well. Cosmic rays are one source of background radiation. Another source is the scattering of ^{137}Cs radiation off of the lead bricks surrounding the apparatus. Fortunately, this noise source will be small compared to the quantity of radiation emitted by the scatterer.

3 Experimental methods

We arranged the scintillation detector and scatterer around the ^{137}Cs radiation source as shown in Figure 3 and as pictured in Figure 4. For data collection, we used the MAESTRO software package.

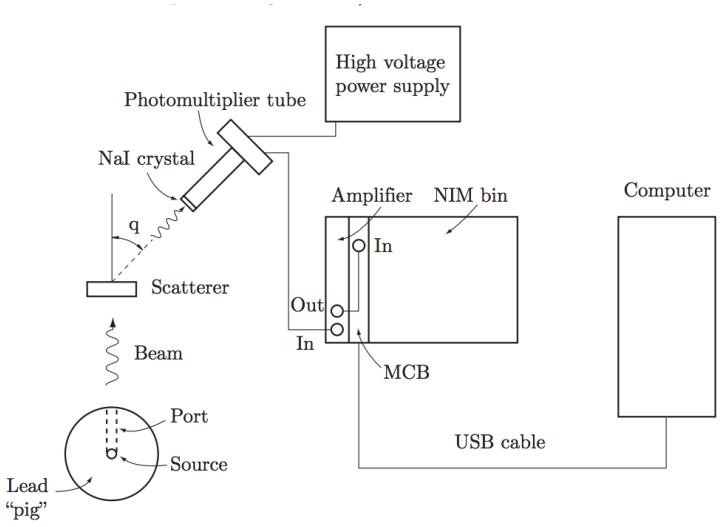

Figure 3: Overview of the experimental setup for the Compton effect, taken from [4]. Lead bricks (not pictured) surround the radiation source and detector to shield apparatus from external radiation.

One important parameter in the experimental setup was the voltage of the high voltage source (see Figure 4). We found that 1000 V was an optimal value. A second important parameter was the gain setting of the amplifier pictured in Figure 3. We found that a gain of 54.4x was optimal. The final important parameter was the distance between the ^{137}Cs source and the nose of the scintillation detector. For distances of less than 0.5 m, our data was very noisy. We found that a distance of 1 m was optimal, as pictured in Figure 4.

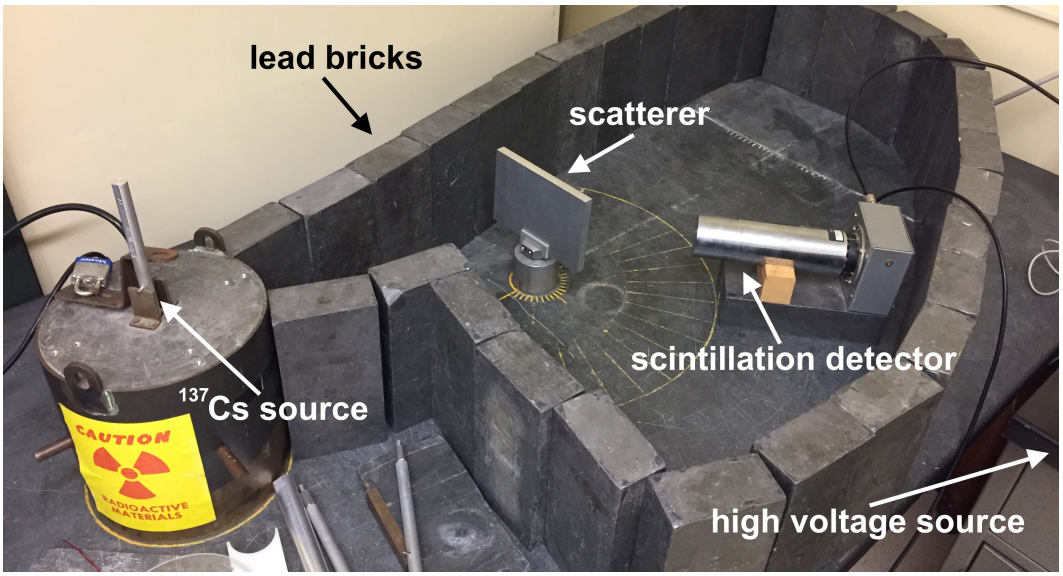

Figure 4: Picture of our actual experimental setup for the Compton effect. Lead bricks surround the radiation source and detector to shield apparatus from external radiation.

To minimize environmental noise, we surrounded the radiation source, scatterer, and scintillation detector with a wall of lead bricks. These reduced environmental noise substantially. We collected data for 180 seconds during both the calibration and scattering portions of the experiments. An overview of the data we took is shown in Table 1.

Source	Run type	Time (s)	ϕ (degrees)	Scattering	Control
^{60}Co	Calibration	180	0		x
^{22}Na	" "	" "	0		x
^{137}Cs	" "	" "	0		x
^{137}Cs	Control	180	0		x
^{137}Cs	" "	" "	10		x
^{137}Cs	" "	" "	20		x
^{137}Cs	" "	" "	30		x
^{137}Cs	" "	" "	40		x
^{137}Cs	" "	" "	50		x
^{137}Cs	Scattering	180	0	x	
^{137}Cs	" "	" "	10	x	
^{137}Cs	" "	" "	20	x	
^{137}Cs	" "	" "	30	x	
^{137}Cs	" "	" "	40	x	
^{137}Cs	" "	" "	50	x	

Table 1: Overview of the data collected. The scattering angle, in degrees, is denoted by ϕ

4 Results and Discussion

4.1 Calibration

In order to assign energy values to bin numbers, we used three different radiation sources: ^{137}Cs, ^{60}Co, and ^{22}Na. Each of these sources gave us at least one peak with a known energy at a different bin number. Combining these peaks and their known energies, we were able to find a linear mapping between bin number x and incident gamma ray energy E_γ.

Shown below are the three plots we used for calibration, one for each radiation source. Each one represents 180 seconds of data collected using the experimental setup described in Section 3.

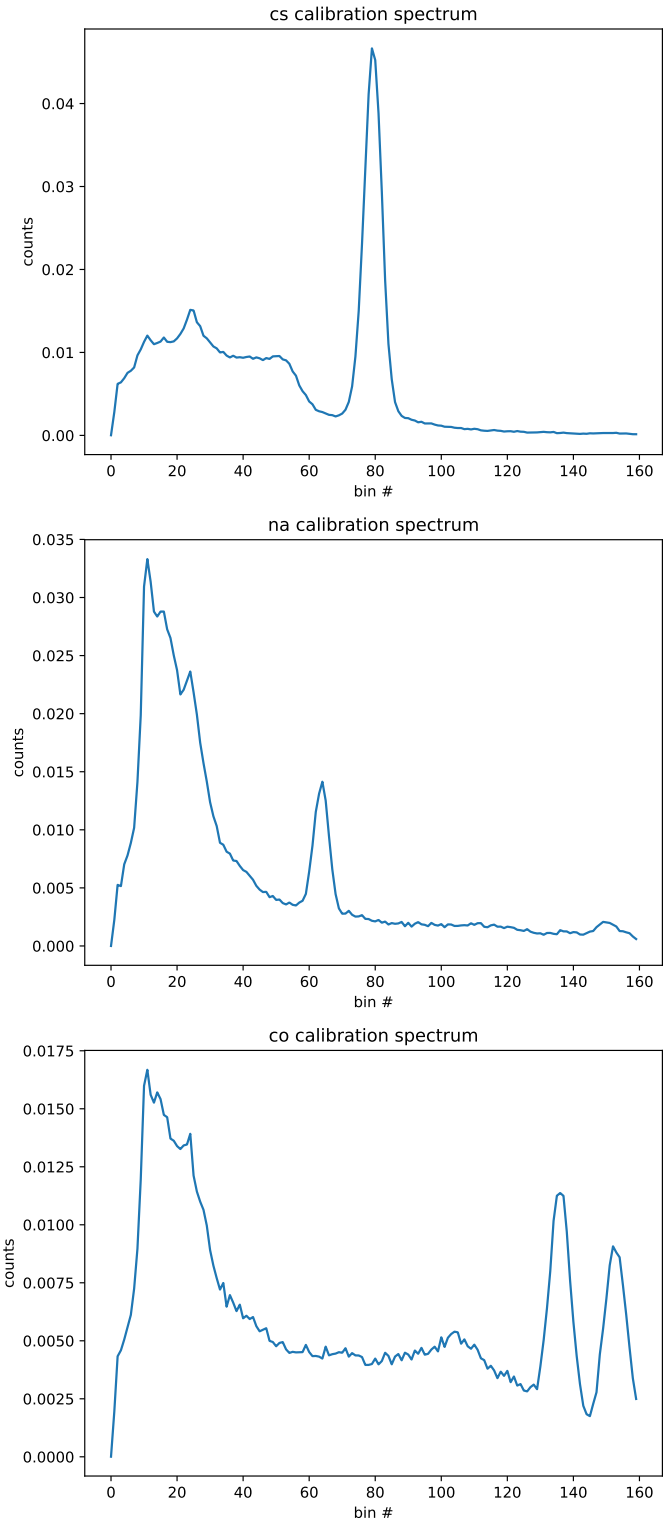

Figure 5: Calibration plots for ^{137}Cs, ^{137}Na, and ^{60}Co (each has been normalized)

Peak finding. To determine the bin numbers corresponding to each of the main peaks, we wrote a simple peak-finding script in Python.

1. Given a threshold, it finds all the bins with values greater than that threshold
2. Next, it uses that information to find all the bins where the inflection from to below-threshold to above-threshold happens
3. It averages the indices of these "inflection" bins in pairs of twos to estimate the center of the peak. This works, as long as the shape of the peak is roughly symmetric

The code is well-documented and available online in a Jupyter notebook *. Having found the principal peaks, we discarded the first peaks for ^{60}Co and ^{22}Na; these peaks correspond to background noise. Next, we looked up the energy (in keV) that corresponded to each of the four remaining peaks. This information is available in any experimental physics textbook or website [3] [4].

Source	Peak energy (keV)	Peak location (bin #)
^{60}Co	1170	135.5
^{60}Co	1330	152.0
^{137}Cs	662	78.5
^{22}Na	511	63.0

Table 2: Peak data

Plotting this relationship, we were able to obtain a very strong linear fit ($r^2 = 0.9998$), shown in Figure 6.

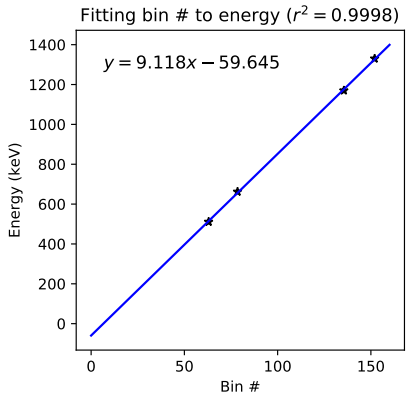

Figure 6: Regression

4.2 Scattering

Having obtained a mapping between bin number and photon energy, we began analysis on the scattering data. On all plots in this section, the x-axes of plots are in units of energy (keV), where the original bin numbers have been scaled by the linear relationship displayed in Figure 6.

First, we plotted scattering spectra against control spectra for scattering angles $\phi = \{0, 10, 20, 30, 40, 50, 60\}$ to determine the overall quality of the data and search for any general trends (Figure 7). It is clear that the spectra are nearly identical. For several of the plots ($\phi = \{0, 10, 20, 30\}$), we observed a slight leftward shift of the 662 keV ^{137}Cs photopeak.

*https://github.com/greydanus/compton

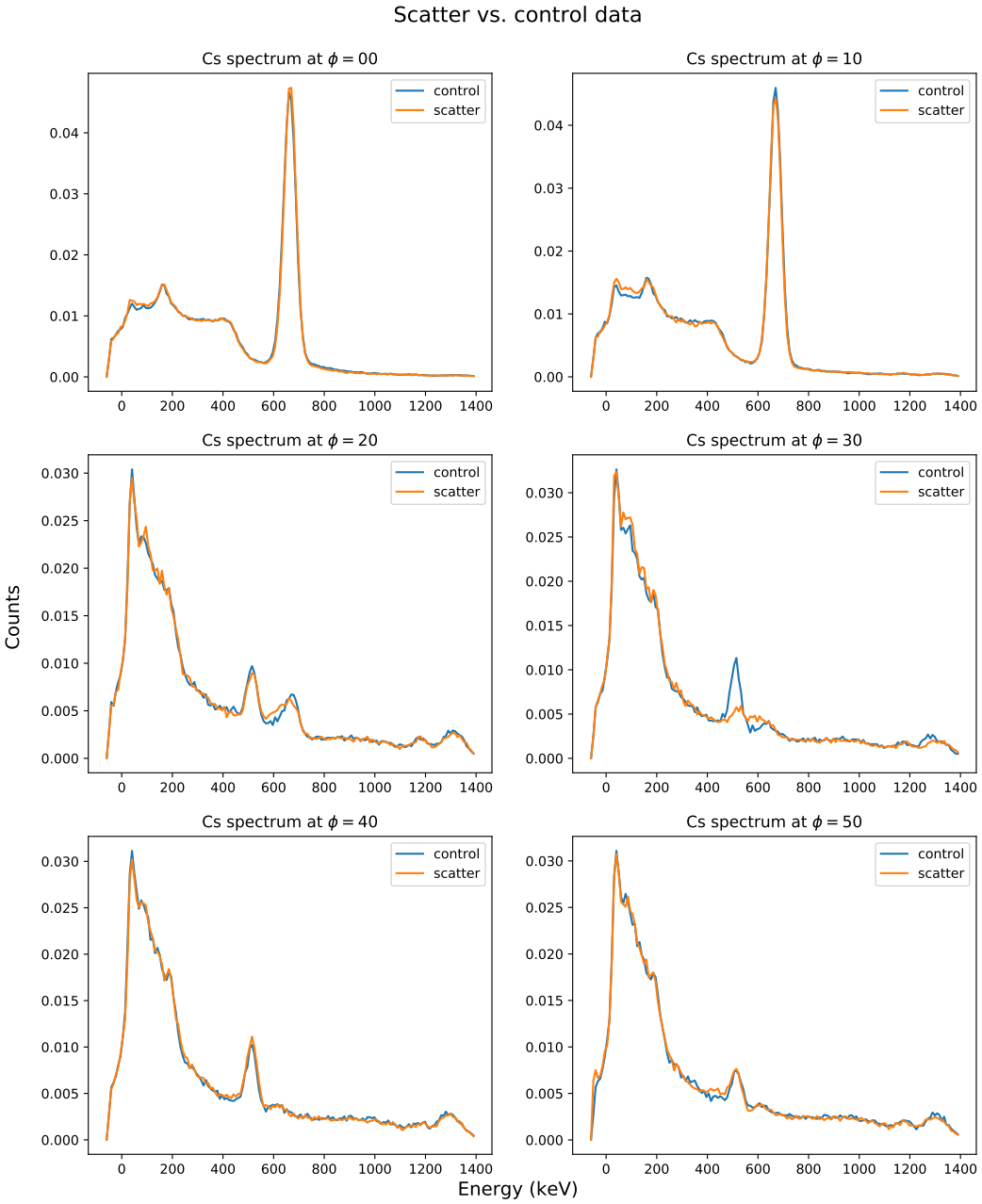

Figure 7: Comparing ^{137}Cs data for scattering and control runs at scattering angles $\phi = \{0, 10, 20, 30, 40, 50, 60\}$. Though the spectra are nearly identical, one can resolve minor leftward shifts of the 662 keV ^{137}Cs photopeak for $\phi = \{0, 10, 20, 30\}$

To better resolve the leftward shift of the 662 keV photopeak, we also plotted differences for $\phi = \{0, 10, 20, 30, 40, 50, 60\}$. As expected, we obtained a large peak followed by a valley in the 662 keV region for several of the plots, corresponding to a slight leftward shift of the peak. These results are shown in 8.

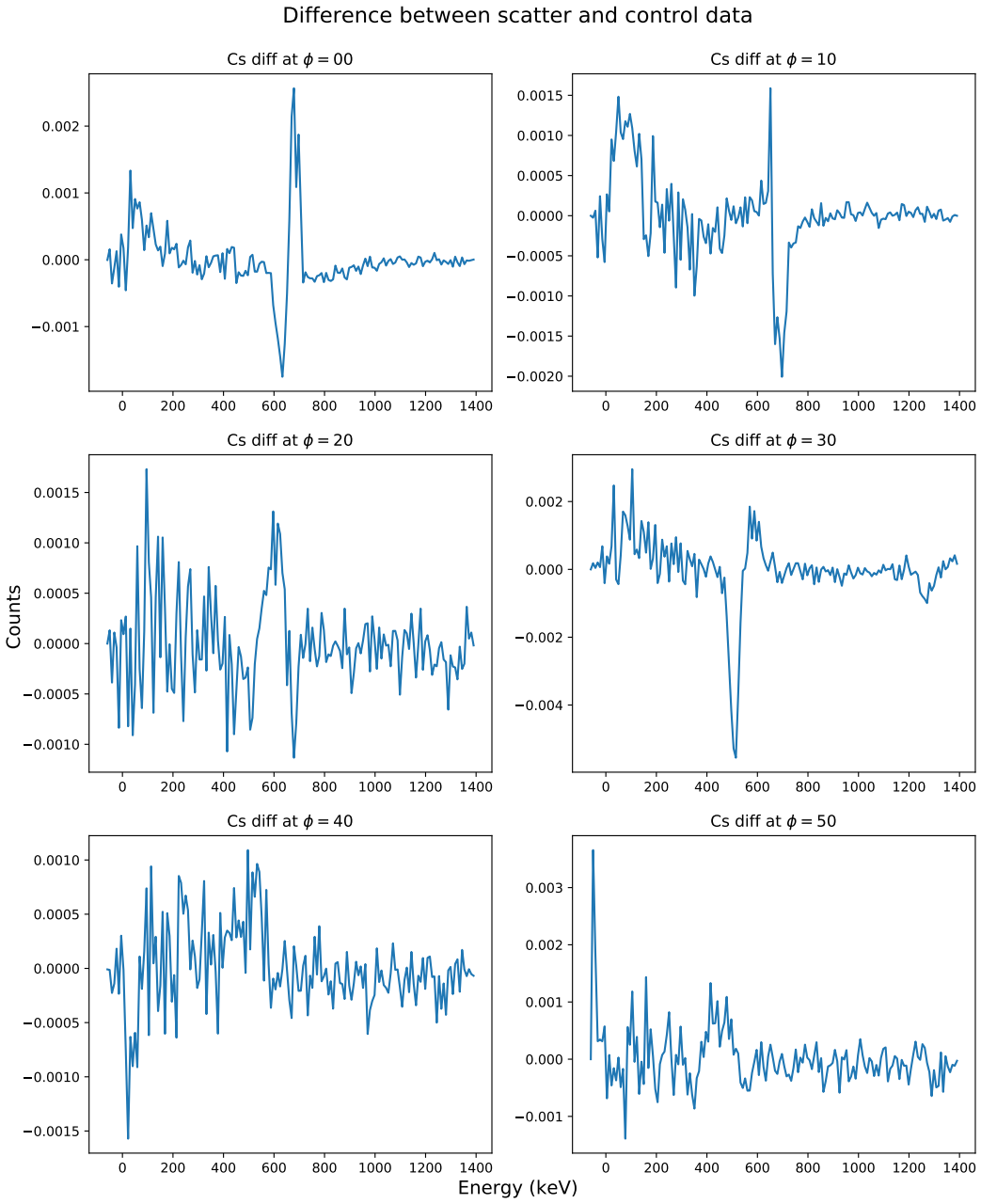

Figure 8: Comparing ^{137}Cs data for difference between scattering and control runs at scattering angles $\phi = \{0, 10, 20, 30, 40, 50, 60\}$. The peak-valley patterns in the 662 keV region correspond to a slight leftward shift ^{137}Cs photopeak due to scattering

Quantify shifts. To quantify the shifts shown in 8, we applied the same peak-finding algorithm to a the difference plots which showed a pronounced shift ($\phi = \{0, 10, 20\}$ because $\phi = 30$ appears to be caused by some other disturbance). The peaks we found correspond to the new photopeak energy of ^{137}Cs, after scattering. Results are shown in 3.

ϕ (degrees)	Photopeak energy
00	669.78
10	642.43
20	615.07

Table 3: ^{137}Cs Photopeak shifts due to Al scattering

Although these results cannot allow us to *directly* verify the theoretical predictions of Section 2, they confirm the hypothesis that gamma rays lose some energy as they pass through a scattering material. This confirms that there is indeed a useful signature in our data. In order to test whether this signature can verify our theoretical predictions, we now need to calculate the ratio N/N_0 from equation 6.

Compare data to theory. We have two theoretical models, the Thomson and the Klein-Nishna differential cross sections (equations 3 and 2 respectively). From the experimental data, we were able to calculate the ratio N/N_0, which changes according to scattering angle ϕ. Then, using equation 6, we solved for $\frac{d\sigma}{\Delta\Omega}$. Now, to compare data to theory, we simply needed to find experimental values of N/N_0. We did this by dividing scattering data by control data for $\phi = \{0, 10, 20, 30, 40, 50, 60\}$ as shown in Figure 9.

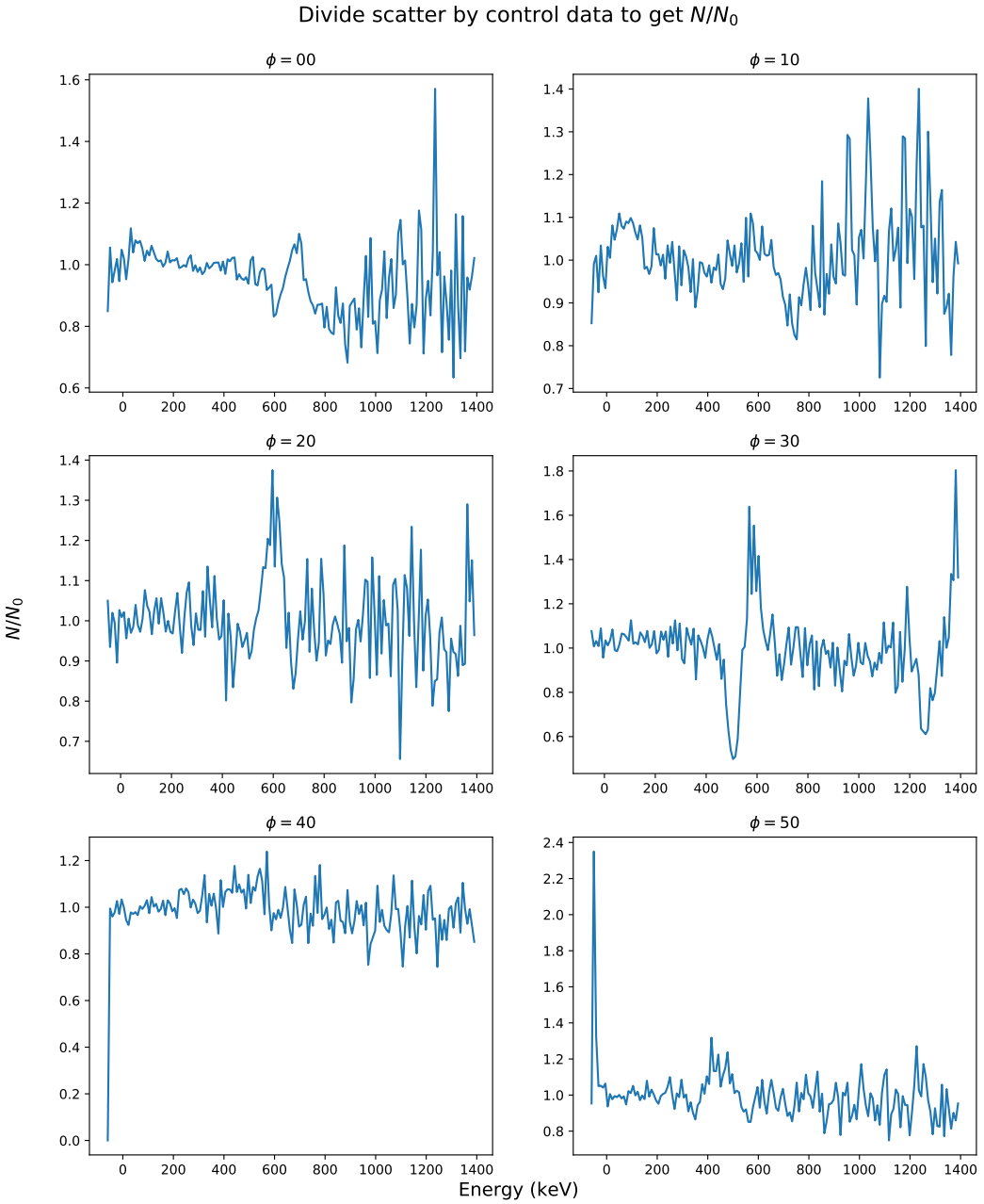

Figure 9: Dividing ^{137}Cs scattering data by control data for scattering angles $\phi = \{0, 10, 20, 30, 40, 50, 60\}$. The data is very messy, so we were forced to make best guesses for the ratio N/N_0 in the 662 keV region.

ϕ (degrees)	N/N_0
00	0.87
10	0.83
20	.85
30	.55

Table 4: The data in 9 is very messy so we were forced to make best guesses for the ratio N/N_0 in the 662 keV region.

Finally, we plotted our experimental estimates of the differential cross section against the two theoretical predictions. We were unable to quantify the error in our experimental data points because the largest source of error was introduced by our "best guess" estimations of the ratio N/N_0. We estimate that our experimental data points are accurate only to the nearest order of magnitude. Even so, these estimates were on the same order of magnitude as the theoretical predictions, as shown in Figure 10.

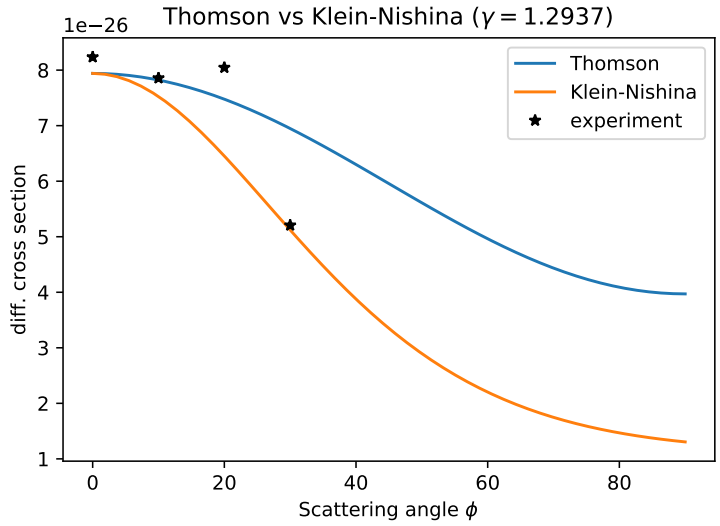

Figure 10: Comparing theoretical predictions of the differential cross section of Compton scattering to experimental results

The code, equations, and figures for conducting this analysis are all available (in far more detail and clarity) online [†].

5 Conclusions

We need more – and better – data to reject Thompson's equation and confirm that the Klein-Nishina equation is a better theoretical model. Even so, our experimental results fall within the same order of magnitude as the theoretical predictions for the differential cross section. Though this is encouraging, we acknowledge that this is probably due in large part to chance.

Taking a large amount of data at the scattering angle of $\phi = 60$ would be particularly useful in future work. For this angle, the predictions of the Thomson equation are very different from those of the Klein-Nishna equation. Given a greater amount of data, we would be able to perform a more rigorous analysis thus resolve this difference with great precision.

In performing experiments to quantify the effects of Compton scattering, we showed that one must treat light as a particle in order to obtain accurate theoretical predictions, thus confirming the quantum

[†] https://nbviewer.jupyter.org/github/greydanus/compton/blob/master/analysis.ipynb

nature of the photon. Had we been able to verify the Klein-Nishina equation, we would also have proven that one must use relativistic calculations to make accurate predictions. We are confident that this can be done with the apparatus described, given more time.

We explored the quantum nature of light with Compton scattering. We showed that photons behave lie particles during the Compton interaction because our results agreed well with the theoretical predictions of Thomson and Klein-Nishina, which treat light as a particle. In this sense, our results constitute a dramatic experimental verification of subatomic theory.

6 Acknowledgements

Special thanks to instructor Kipp van Schooten and teaching assistants Yanping Cai and Lihuang Xu for always guiding us in the right direction.

References

[1] Arthur H Compton. A Quantum Theory of the Scattering of X-Rays By Light Elements. *The Physical Review*, 21(5):483–502, 1923.

[2] O. Klein and Y. Nishina. On the scattering of radiation by free electrons according to the new relativistic quantum dynamics of Dirac. *Zeitschrift für Physik*, 52(11-12):853–868, nov 1929.

[3] P. Magdziarz and A. A. Zdziarski. Angle-dependent Compton reflection of X-rays and gamma-rays. *Mnras*, 273(3):837–848, 1995.

[4] Kipp van Schooten. Compton Scattering. Technical Report 1, Dartmouth College, Hanover, 2017.